

# Structural, Electronic and Optical Properties of 2D Monolayer and Bilayer CoO<sub>2</sub>

V.R. Patel<sup>1,a\*</sup>, A.R. Patel<sup>1,b</sup>, Yogesh Sonvane<sup>2,c</sup> and P.B. Thakor<sup>1,d</sup>

<sup>1</sup>Department of Physics, Veer Narmad South Gujarat University, Surat, 395007, India

<sup>2</sup>Department of Applied Physics, S.V. National Institute of Technology, Surat 395007, India

<sup>a</sup>varsha0127@gmail.com, <sup>b</sup>arpatel14@hotmail.com, <sup>c</sup>yas@phy.svnit.ac.in,

<sup>d</sup>pbthakor@rediffmail.com

**Keywords:** Monolayer, Bilayer, Electronic Properties, First-Principles Calculations, Optical Properties

**Abstract.** In present study, structural, electronic, and optical absorption properties of two dimensional (2D) monolayer and bilayer CoO<sub>2</sub> have been calculated by using the density functional theory. From the electronic band-structures of monolayer CoO<sub>2</sub> and bilayer CoO<sub>2</sub>, these materials show metallic (conducting) behavior. The Optical absorption of monolayer and bilayer CoO<sub>2</sub> begins from the infrared region to visible region and maximum absorption in ultraviolet region of the electromagnetic spectrum. Results suggest that the monolayer and bilayer CoO<sub>2</sub> may be utilized for the optoelectronic applications and nano electronics.

## Introduction

The discovery of graphene, gives completely new era of two dimensional materials[1]. Since the invention of the exotic properties of graphene, the two-dimensional layer materials like transition metal oxides (TMO), transition metal-dichalcogenides (TMDs), and other 2D materials have gained enormous research interest [2]. Cobalt oxide (CoO<sub>2</sub>) is an end member of A<sub>x</sub>CoO<sub>2</sub> (A = Li, Na), which is the auspicious material as cathode for fabrication of lithium ion batteries that was studied in previous investigation [3–9]. CoO<sub>2</sub> is an adaptable metal oxide material having many applications in various fields such as catalyst, electrochemical biosensor, photocatalyst and other applications [10]. First principles computations are used to study structural, electrical, and optical absorption properties of two-dimensional (2D) monolayer and bilayer CoO<sub>2</sub>.

## Computational Details

In the present work, all the calculations have been performed by the density functional theory (DFT). We have been used the generalized gradient approximation (GGA) as employed in QUANTUM ESPRESSO (QE) package with Perdew, Burke and Ernzerhof (PBE) pseudopotential [11,12]. For both the energy cut-off and the k-points, we have followed the convergence criteria. The structure was relaxed toward its equilibrium position, with the force on each atom being less than 10<sup>-5</sup> Ry/Bohr. The energy cutoff for the wave functions was chosen as 80 Ry. The self-consistent calculations are performed with a Monkhorst-Pack of 15x15x1 k-mesh is used [13]. To avoid physical interaction between the periodic layers, a vacuum of order 18 Å in z-direction was utilized. VESTA software was utilized for the visualization of the optimized structure [14].

## Results and Discussion

### Structural Properties

The optimized structures of monolayers and bilayer of  $\text{CoO}_2$  are shown in Fig. 1. The two-dimensional hexagonal lattice, monolayer  $\text{CoO}_2$  with the lattice parameters of  $a = 2.870 \text{ \AA}$  and,  $b = 2.870 \text{ \AA}$  and the bond-length for the bonds Co-O is  $1.91 \text{ \AA}$ , which is consistent with previous reported work [4]. In bilayer  $\text{CoO}_2$  with lattice parameters of  $a = 2.874 \text{ \AA}$ , and  $b = 2.874 \text{ \AA}$  (see Table 1) and, the bond-length for the bonds Co-O is  $1.91 \text{ \AA}$ . The monolayer and bilayer  $\text{CoO}_2$  have positive phonon frequencies which indicates that both are dynamically stable [15].

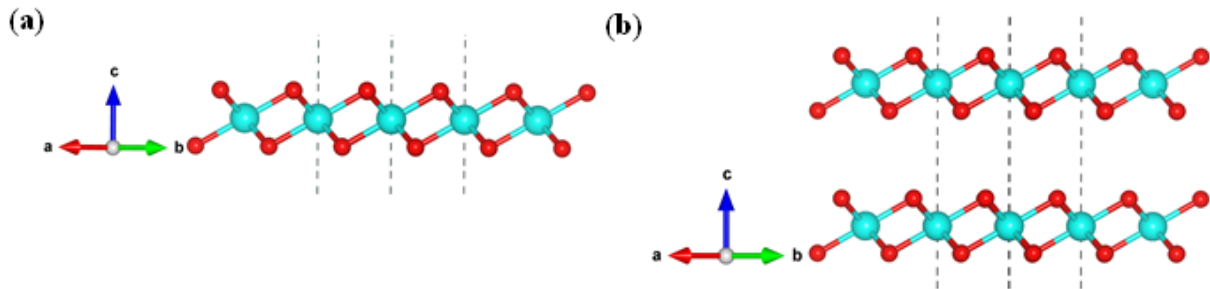


Fig. 1. The optimized structure of (a) Side view of monolayer  $\text{CoO}_2$  (b) Side view of bilayer  $\text{CoO}_2$ .

Table 1. Calculated the lattice-parameters and bond-length of the monolayer and bilayer  $\text{CoO}_2$

Structure	Lattice Constants		Bond length ( $\text{\AA}$ )
	a ( $\text{\AA}$ )	b ( $\text{\AA}$ )	
Monolayer $\text{CoO}_2$	2.870	2.870	Co-O 1.91
Bilayer $\text{CoO}_2$	2.874	2.874	Co-O 1.91

### Electronic properties

Fig. 2a and Fig. 2b shows the electronic band structures of the monolayer and bilayer  $\text{CoO}_2$  along the k-path  $\Gamma - \text{M} - \text{K} - \Gamma$ . In monolayer and bilayer  $\text{CoO}_2$  both exhibits metallic characteristics when both the bands cross the Fermi-level. In monolayer  $\text{CoO}_2$  the position of the valance-band maximum, and the conduction-band minimum are found at  $\Gamma$  point. Projected density of states (PDOS) for monolayer, and bilayer  $\text{CoO}_2$  are illustrated in Fig. 2c and Fig. 2d. The Co(d) orbital and O(p) orbital shows more contributions and less contributions of the O(d) orbital for the creation of the valance-band (VB) and the O(d) orbital gives less contributions for the creation of the conduction-band (CB) in monolayer  $\text{CoO}_2$ . The Co(d) orbital and the O(p) orbital shows more contributions and the O(d) orbital shows less contributions for the creation of the valance-band (VB) and the Co(d) orbital and the O(p) shows more contributions and the O(d) orbital shows less contributions for the creation of the conduction-band (CB) in bilayer  $\text{CoO}_2$ . The metallic behaviour of monolayer and bilayer  $\text{CoO}_2$  is because of hybridization of the Co(d) orbital, and the O(p) orbital.

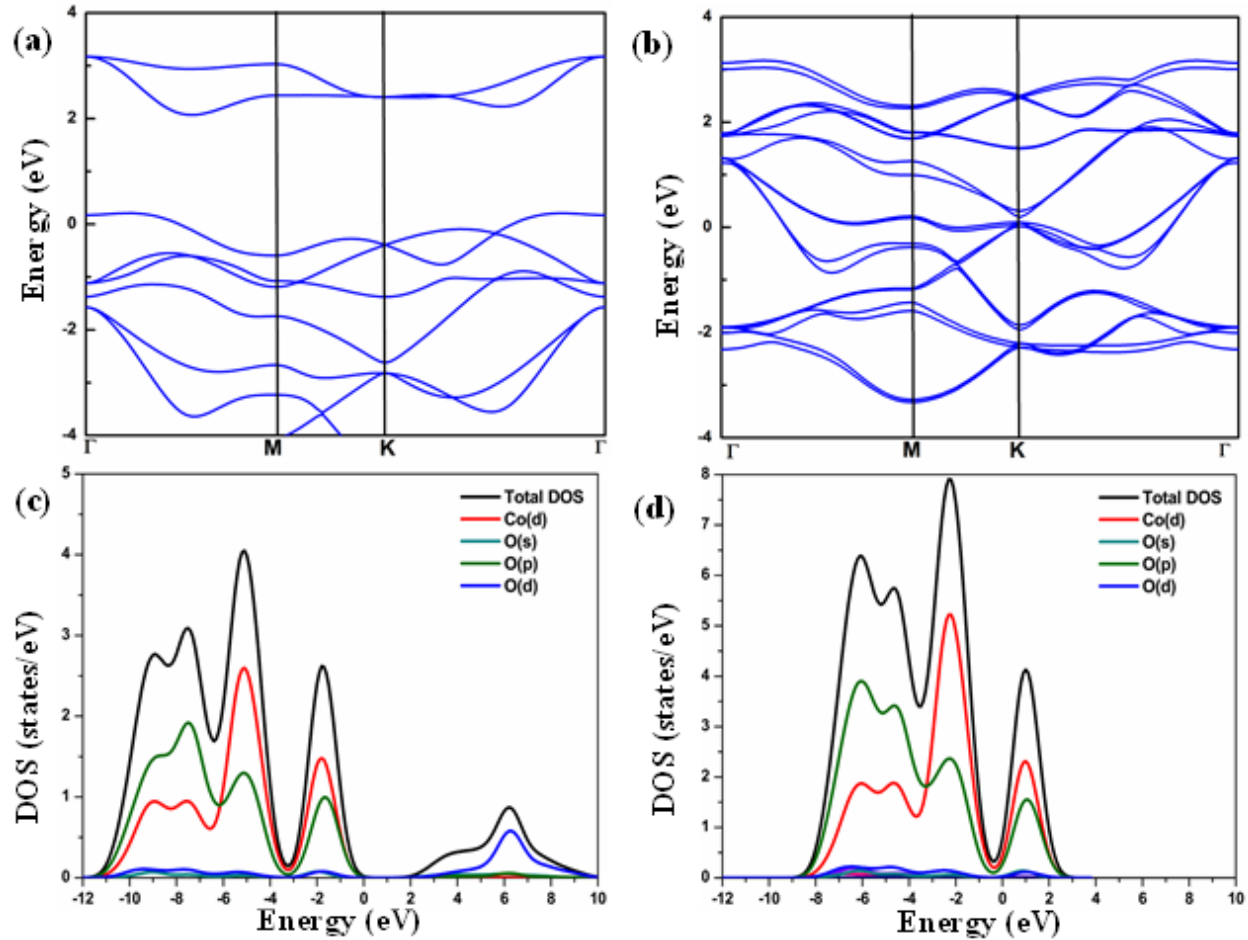


Fig. 2. (a) Band-structure of monolayer  $\text{CoO}_2$  (b) Band-structure of bilayer  $\text{CoO}_2$  (c) PDOS of monolayer  $\text{CoO}_2$  (d) PDOS of bilayer  $\text{CoO}_2$

### Optical Properties

For study the optical properties of monolayer and bilayer  $\text{CoO}_2$  we have calculated the absorption coefficients. Fig. 3 illustrates the optical absorption spectra of monolayer and bilayer  $\text{CoO}_2$ . The first absorptions peaks are observed in visible region for monolayer and bilayer  $\text{CoO}_2$ . Furthermore, the photon energies that correspond to the first absorption peaks located at 1.98 eV, and 1.92 eV for monolayer  $\text{CoO}_2$ , and bilayer  $\text{CoO}_2$ . The maximum absorption peak values are observed at 7.59 eV and, 7.53 eV, respectively, as shown in Fig. 3, which both are lies in the ultraviolet (UV) region for monolayer and bilayer  $\text{CoO}_2$ , respectively. The optical absorption of monolayer  $\text{CoO}_2$  is slightly less than that of bilayer  $\text{CoO}_2$ . It is observed that optical absorption of monolayer and bilayer  $\text{CoO}_2$  begins from the infrared (IR) region to visible region and shows maximum absorption in the ultraviolet regions of the electromagnetic spectrum. The results indicate that, optical absorption in visible region to ultraviolet region in monolayer  $\text{CoO}_2$  and bilayer  $\text{CoO}_2$  so that it can be used for optoelectronic applications.

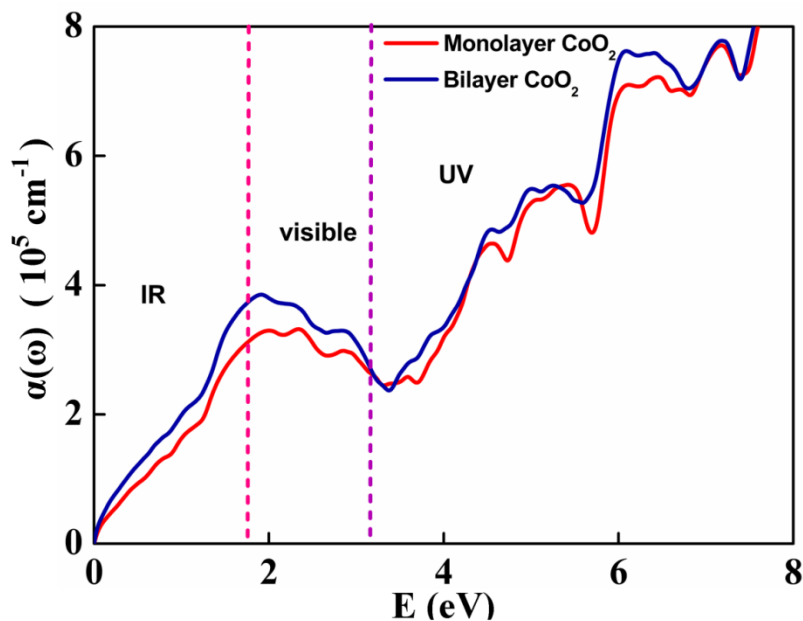


Fig. 3. Optical absorption spectra of monolayer and bilayer CoO<sub>2</sub>

### Conclusions

We have investigated structural, electronic, and optical absorption properties of two dimensional monolayer and bilayer CoO<sub>2</sub> in the present study. From the calculation of the electronic-band structures of monolayer, and bilayer CoO<sub>2</sub>, these materials show metallic (conducting) behavior. The optical absorption spectra of the monolayer and bilayer CoO<sub>2</sub> have large absorption in visible region to ultraviolet region of electromagnetic spectrum. Results suggest that the monolayer and bilayer CoO<sub>2</sub> may be useful in the optoelectronic applications and nano electronics.

### References

- [1] M. Xu, T. Liang, M. Shi, H. Chen, Graphene-like two-dimensional materials, *Chem. Rev.* 113 (2013) 3766–3798. <https://doi.org/10.1021/cr300263a>
- [2] C. Chowdhury, S. Karmakar, A. Datta, Monolayer Group IV-VI Monochalcogenides: Low-Dimensional Materials for Photocatalytic Water Splitting, *J. Phys. Chem. C.* 121 (2017) 7615–7624. <https://doi.org/10.1021/acs.jpcc.6b12080>
- [3] G.G. Amatucci, J.M. Tarascon, L.C. Klein, CoO<sub>2</sub>, The End Member of the Li<sub>x</sub>CoO<sub>2</sub> Solid Solution, *J. Electrochem. Soc.* 143 (1996) 1114–1123. <https://doi.org/10.1149/1.1836594>
- [4] T. Motohashi, Y. Katsumata, T. Ono, R. Kanno, M. Karppinen, H. Yamauchi, Synthesis and Properties of CoO<sub>2</sub>, the x = 0 End Member of the Li<sub>x</sub>CoO<sub>2</sub> and Na<sub>x</sub>CoO<sub>2</sub> Systems. , *Chem. Mater.* 19 (2007) 5202–5202. <https://doi.org/10.1021/cm702533v>
- [5] T. Motohashi, T. Ono, Y. Katsumata, R. Kanno, M. Karppinen, H. Yamauchi, Electrochemical synthesis and properties of CoO<sub>2</sub>, the x=0 phase of the A<sub>x</sub>CoO<sub>2</sub> systems (A=Li,Na), *J. Appl. Phys.* 103 (2008). <https://doi.org/10.1063/1.2828525>
- [6] M. Onoda, A. Sugawara, Stacking faults and metallic properties of triangular lattice CoO<sub>2</sub> with a three-layer structure, *J. Phys. Condens. Matter.* 20 (2008). <https://doi.org/10.1088/0953-8984/20/17/175207>

- [7] K.W. Lee, W.E. Pickett,  $\text{Na}_x\text{CoO}_2$  in the  $x \rightarrow 0$  regime: Coupling of structure and correlation effects, *Phys. Rev. B - Condens. Matter Mater. Phys.* 72 (2005) 1–7. <https://doi.org/10.1103/PhysRevB.72.115110>
- [8] E.B. Isaacs, C.A. Marianetti, Compositional phase stability of correlated electron materials within DFT+DMFT, *Phys. Rev. B.* 102 (2020) 1–11. <https://doi.org/10.1103/PhysRevB.102.045146>
- [9] H. Kang, J. Lee, T. Rodgers, J.H. Shim, S. Lee, Electrical Conductivity of Delithiated Lithium Cobalt Oxides: Conductive Atomic Force Microscopy and Density Functional Theory Study, *J. Phys. Chem. C.* 123 (2019) 17703–17710. <https://doi.org/10.1021/acs.jpcc.9b03232>
- [10] M. Ranjbar, Thermal decompose method for synthesis and characterization of  $\text{CoO}_2/\text{GrO}$  nanostructures and optical investigation, *J. Mater. Sci. Mater. Electron.* 27 (2016) 11707–11712. <https://doi.org/10.1007/s10854-016-5307-6>
- [11] P. Giannozzi, S. Baroni, N. Bonini, M. Calandra, R. Car, C. Cavazzoni, D. Ceresoli, G.L. Chiarotti, M. Cococcioni, I. Dabo, A. Dal Corso, S. De Gironcoli, S. Fabris, G. Fratesi, R. Gebauer, U. Gerstmann, C. Gougoussis, A. Kokalj, M. Lazzeri, L. Martin-Samos, N. Marzari, F. Mauri, R. Mazzarello, S. Paolini, A. Pasquarello, L. Paulatto, C. Sbraccia, S. Scandolo, G. Sclauzero, A.P. Seitsonen, A. Smogunov, P. Umari, R.M. Wentzcovitch, QUANTUM ESPRESSO: A modular and open-source software project for quantum simulations of materials, *J. Phys. Condens. Matter.* 21 (2009). <https://doi.org/10.1088/0953-8984/21/39/395502>
- [12] J.P. Perdew, K. Burke, M. Ernzerhof, Generalized Gradient Approximation Made Simple, *Phys. Rev. Lett.* 77 (1996) 3865–3868. <https://doi.org/10.1103/PhysRevLett.77.3865>
- [13] H.J. Monkhorst, J.D. Pack, Special points for Brillouin-zone integrations, *Phys. Rev. B.* 13 (1976) 5188–5192. <https://doi.org/10.1103/PhysRevB.13.5188>
- [14] K. Momma, F. Izumi, VESTA 3 for three-dimensional visualization of crystal, volumetric and morphology data, *J. Appl. Crystallogr.* 44 (2011) 1272–1276. <https://doi.org/10.1107/S0021889811038970>
- [15] D.L. Nguyen, C.R. Hsing, C.M. Wei, Theoretical prediction of superconductivity in monolayer  $\text{CoO}_2$ , *Nanoscale.* 11 (2019) 17052–17057. <https://doi.org/10.1039/C9NR03954F>